Available online at BCREC website: https://bcrec.id

Bulletin of Chemical Reaction Engineering & Catalysis, 18 (4) 2023, 700-712

Research Article

Bimetallic Ru-Sn as Effective Catalysts for the Selective Hydrogenation of Biogenic Platform Chemicals at Room Temperature

Atina Sabila Azzahra[1], Heny Puspita Dewi[1], Edi Mikrianto[1,2], Kiky Corneliasari Sembiring[3], Gagus Ketut Sunnardianto[4], Iryanti Fatyasari Nata[5], R. Rodiansono[1,2,6,*], J. Jayanudin[6,7]

[1]Inorganic Materials and Catalysis (IMCat), Catalysis for Sustainable Energy & Environment (CATSuRe), Lambung Mangkurat University, 70714, Indonesia.
[2]Department of Chemistry, Lambung Mangkurat University, Jl. A. Yani Km 36 Banjarbaru, 70714, Indonesia.
[3]Centre for Advanced Chemistry, BRIN, KST BJ Habibie Serpong, Tangerang, Indonesia.
[4]Research Centre for Quantum Physics, BRIN, KST BJ Habibie Serpong, Tangerang, Indonesia.
[5]Department of Chemical Engineering, Lambung Mangkurat University, Jl. A. Yani Km 35 Banjarbaru, 70714, Indonesia.
[6]Research Collaboration Center for Tin Metal, Faculty of Engineering, Universitas Sultan Ageng Tirtayasa, Jl. Jenderal Sudirman Km 3, Cilegon, Indonesia.
[7]Department of Chemical Engineering, Faculty of Engineering, Universitas Sultan Ageng Tirtayasa, Jl. Jenderal Sudirman Km 3, Cilegon, Indonesia.

Received: 31st October 2023; Revised: 21st November 2023; Accepted: 27th November 2023
Available online: 29th November 2023; Published regularly: December 2023

Abstract

Supported bimetallic ruthenium-tin (denoted as Ru-Sn(x); x = molar ratio of Ru/Sn) catalysts were examined for room temperature (RT) hydrogenation of biogenic platform chemicals of levulinic acid (LA) to γ–valerolactone (GVL). Six types of metal oxide support *c.a.* Nb_2O_5, TiO_2, ZnO, ZrO_2, γ–Al_2O_3, active charcoal (AC), were employed as the support for Ru-Sn(x). Ru-Sn(3.0)/Nb_2O_5 (Ru/Sn = 3.0) that reduced at 500 °C demonstrated the highest yield of GVL (98%) at 30 °C, 30 bar H_2 for 3 h. The increase in Sn loading amount (Ru/Sn = 1.5) resulted in decreasing of LA conversion (83%) under the same reaction conditions. Among the studied supported Ru-Sn catalysts, Nb_2O_5 and ZnO supports exhibited better catalytic performances than that other for RT hydrogenation of LA and various biogenic platform chemicals. The Ru-Sn(3.0)/Nb_2O_5 catalyst was characterized by means of various adsorption and spectroscopic techniques. The Ru-Sn(3.0)/Nb_2O_5 catalyst was found to be reusable without any significant loss of its activity.

Copyright © 2023 by Authors, Published by BCREC Group. This is an open access article under the CC BY-SA License (https://creativecommons.org/licenses/by-sa/4.0).

Keywords: bimetallic ruthenium-tin; room temperature hydrogenation; biogenic platform chemicals; levulinic acid; γ-valerolactone

How to Cite: A.S. Azzahra, H.P. Dewi, E. Mikrianto, K.C. Sembiring, G.K. Sunnardianto, I.F. Nata, R. Rodiansono, J. Jayanudin (2023). Bimetallic Ru-Sn as Effective Catalysts for the Selective Hydrogenation of Biogenic Platform Chemicals at Room Temperature. *Bulletin of Chemical Reaction Engineering & Catalysis*, 18(4), 700-712 (doi: 10.9767/bcrec.20067)

Permalink/DOI: https://doi.org/10.9767/bcrec.20067

1. Introduction

The dwindling supplies of fossil fuels supply and the increasing of the energy demand, lignocellulosic biomass possesses the promising feedstocks that can be converted into various chemicals and fuel platforms using acid catalyst [1,2]. For instance, a biomass consist of C5-C6 sugars can be transformed into oxygenates such as furfural (FFald), levulinic acid (LA), and various organic carboxylic acids [3–5].

* Corresponding Author.
Email: rodiansono@ulm.ac.id (R. Rodiansono);

Among those oxygenates, LA is perhaps the most interesting platform chemical as it can be made in relatively high yields from lignocellulosic by using diluted sulfuric acid catalyst [6], which could be turned out into various high-added value chemicals and fuels in the presence of heterogeneous bimetallic catalysts [7]. Under low temperature, the hydrogenation of LA leads to the formation of γ–hydroxyvaleric acid (GHVA) as an unstable intermediate then undergoes to ring closure by intermolecular esterification and loses a water molecule to form γ–valerolactone (GVL) [8] or dehydration to form α–angelica lactone (α-AGL), which is followed by hydrogenation to GVL [9]. GVL can be used as versatile feedstock for the synthesis of fuel additives/biofuels [10] (*e.g.,* liquid hydrocarbon diesel [11], gasoline-like hydrocarbon [12], and valeric biofuels [13]), as a precursor of bulk chemicals (*e.g.,* 1,4-pentanediol [14], aromatic hydrocarbon [15], and 4-hydroxyvaleric acid ionic liquids [16]). Furthermore, GVL has been demonstrated to be a renewable solvent for the Sonogashira reaction [17] and a green polar aprotic solvent for the improvement of biomass conversion [18].

Supported ruthenium-based catalysts, in the forms both monometallic and bimetallic systems, have been employed for the catalytic conversion of LA to GVL [19]. Although ruthenium-based catalysts are effective and frequently applied, harsh reaction conditions (at >140 °C and >40 bar of H_2) are required to achieve complete reaction with >99% yield of GVL [20,21]. Only few reports have been published for the catalytic conversion of LA to GVL over Ru-based catalysts at near ambient or low temperature [22]. In the literature, the first established catalyst for the room temperature (RT) hydrogenation of LA to GVL was PtO_2 under high H_2 pressure (≥50 bar) and long reaction time of 40 h with a slow reaction rate of GVL formation [23]. To circumvent these shortcomings, Tan *et al.* [24] developed the Ru/RGO (RGO = reduced graphene oxide) catalysts for RT hydrogenation of LA to GVL with high yield of 99.9% at 40 bar H_2 for 8 h and the highest TOF was 2112 h^{-1}. They suggested that the high activity could be attributed to the formation of electron-rich state of Ru^0 nanoparticles that are demonstrated to be highly active towards the activation of C=O bonds [24]. Consistent with the results of Ru/RGO catalysts, the Ru/FLG (FLG = few-layer graphene) catalysts demonstrated an improved activity, selectivity, and stability compared with Ru/AC and the average GVL production rate was 178 h^{-1} at 40 bar H_2 for 12 h [25]. Moreover, Ru/N-doped hierarchically porous carbon (NHPC) [26] and Ru@C-Al_2O_3 [27] catalysts were examined for RT hydrogenation of LA to GVL (25 °C, 10 bar H_2 and 4-5 h) with the highest TOF of 338 h^{-1} and 658 h^{-1}, respectively. They claimed that these high TOFs were attributed to the strong interaction between Ru^0 and the defect sites of NHPC or C-Al_2O_3 composite which enhanced the activity and prevented the migration and aggregation of Ru nanoparticles. Recently, Ru/TiO_2-nanosheet [28], and Ru/TiO_2@nitrogen doped-carbon (NC) [29] catalysts were applied for RT hydrogenation of LA to GVL (30 °C, 30-60 bar, 8-12 h) with high GVL selectivity and the obtained TOFs were 41.5 h^{-1} and 278 h^{-1}, respectively. The high activity and stability of these catalysts were due to a high dispersion of Ru nanoparticles on TiO_2 nanosheet with exposed (001) facets on TiO_2@CN support. Though both carbon and titania supported Ru-based catalysts were highly active for RT hydrogenation of LA to GVL, they hold the disadvantage of high price of precursors and difficulty in preparing catalyst materials or high initial H_2 pressure used or longer reaction time, thus they may have shortcomings for industrial implementations.

Apart from the development of carbon or titania-supported Ru nanoparticles catalysts, the addition of second electropositive metals (*e.g.,* Sn, In, or Fe) or direct modification of Ru nanoparticles with oxophilic metal oxide species (*e.g.,* ReO_x, WO_x, or MoO_x) have been investigated and applied for various catalytic systems [14,30–32]. Wettstein *et al.* [33] reported carbon supported bimetallic Ru-Sn (Ru-Sn/C) catalysts for selective hydrogenation of LA to GVL in 2-sec-butyl-phenol solvent at quite high pressure and temperature reaction (180 °C and 35 bar H_2). The catalyst containing equal amounts of Ru and Sn had a lower activity for LA to GVL. The beneficial effect of Sn to Ru/C was the increase in activity and stability due to the formation of Ru_2Sn_3 and Ru_3Sn_7 alloy phases [33]. Vorotnikov *et al.* [34] developed an inverse bimetallic RuSn catalyst for selective reduction of carboxylic acids to alcohols. The authors suggested that the SnO_x/Ru species was believed to be responsible for the C–OH scission (SnO_x cluster) and hydrogenation activation (Ru), led to high selectivity of 1-propanol in the hydrogenation of propionic acid at 160 °C, 100 bar H_2 in a trickle bed flow reactor system [34]. Most recently, Ru-Sn/ZnO catalyst was employed for hydrogenation of octanoic acid to octanol in a fixed-bed continuous reactor system at elevated temperatures (300 °C) and 30 bar H_2. The presence of Ru_3Sn_7 al-

Copyright © 2023, ISSN 1978-2993

loy phase was the active site for the significant improvement of the hydrogenation activity and selectivity to octanol as well as the stability in long-term reactions [35].

Herein, we reported the synthesis of supported bimetallic ruthenium-tin (Ru-Sn) by using coprecipitation-hydrothermal method at 150 °C for 24 h, followed by reduction with H_2 at 400-500 °C for 2 h [14,31,32] and applied for the aqueous phase hydrogenation of LA to GVL at room temperature (RT) (Scheme 1). Various metal oxides such as niobium oxide (Nb_2O_5), anatase titanium oxide (TiO_2), zinc oxide (ZnO), zirconia oxide (ZrO_2), and gamma-alumina (γ–Al_2O_3), and active charcoal (AC) were employed for the support of bimetallic ruthenium-tin (denoted as Ru-Sn(x)/support (x = molar ratio of Ru/Sn) catalysts. We found that the Ru-Sn(3.0)/Nb_2O_5 exhibited the highest yield of GVL (98%) with tuneable high Turnover Frequency (TOF) (306 h^{-1}) at 30 °C, 30 bars H_2 after 3 h. The effect of Sn loading amount (Ru/Sn molar ratio), temperature of catalyst reduction, effect of solvent, simple kinetic studies, role of support and catalyst structure-activity relationship are systematically discussed.

2. Materials and Methods

2.1 Materials

Ruthenium(III) chloride ($RuCl_3$) and tin(II) chloride dihydrate ($SnCl_2.2H_2O$) were purchased from Sigma-Aldrich Co. The commercial Ru(5 wt%)/C catalyst was purchased and used as received from Tokyo Chemical Industries Co. The supports of Nb_2O_5, ZnO, ZrO_2, TiO_2 (S_{BET} = 51 $m^2.g^{-1}$), and γ-Al_2O_3 (S_{BET} = 100 $m^2.g^{-1}$) were purchased from Japan Aerosil Co. The active charcoal (AC) (S_{BET} = 600 $m^2.g^{-1}$) was purchased from Merck Millipore co. All organic chemical compounds were purified using standard procedures prior to use [36].

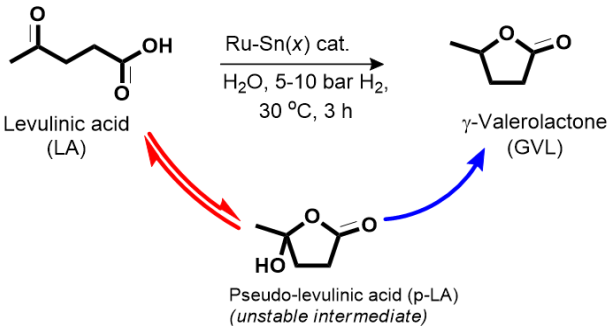

Scheme 1. Reaction pathways for aqueous phase hydrogenation of LA to GVL over bimetallic ruthenium-tin catalysts at room temperature.

2.2 Methods

2.2.1 Catalyst preparation

The detail procedure for the synthesis of bimetallic ruthenium-tin supported on Nb_2O_5 (denoted as Ru-Sn(x)/Nb_2O_5 (x = Ru/Sn molar ratio)) is described as follows [14,31]. Typically, a 0.1025 g (0.494 mmol) $RuCl_3$ (Mr = 207.42; Sigma-Aldrich, 99.9%) was dissolved in deionised water (denoted as solution A) and an ethanol solution of $SnCl_2.2H_2O$ (0.0163 mmol) was dissolved in ethanol (denoted as solution B). A 20 mL ethylene glycol, a 1.0 g Nb_2O_5 (Wako Pure Chemical) and solution A and B were mixed in room temperature and the temperature was raised to 50 °C under gentle stirring for overnight. The mixture then transferred into a teflon with stainless cover of autoclave reactor for hydrothermal treatment at 150 °C for 24 h. A black solid then was calcined with N_2 (200 mL/min) at temperature 30-500 °C for 2 h (ramping 4 °C/min) followed by reduction with H_2 (200 mL/min) at 500 °C for 2 h and produced a reduced Ru-Sn(3.0)/Nb_2O_5 catalyst (3.0 is molar ratio of Ru/Sn).

2.2.2 Catalyst characterizations

The powder X-ray diffraction (XRD) analysis was performed on a Miniflex II 600 Rigaku instrument with Cu as monochromatic source of CuKα radiation (λ = 0.1544 nm). The XRD was operated at 40 kV and 15 mA with a step width of 0.02°, a scan speed of 4°.min^{-1} (α1 = 0.1540 nm, α2 = 0.1544 nm), solar slit 1.25°, and using a Ni Kβ filter.

The Brunauer–Emmett–Teller (BET) specific surface area (S_{BET}) and pore volume (V_p) were measured using N_2 physisorption at -196 °C on a Belsorp Max (BEL Japan). The samples were degassed at 200 °C for 2 h to remove physisorbed gases prior to the measurement. The amount of nitrogen adsorbed onto the samples was used to calculate the specific surface area via the BET equation. The pore volume was estimated to be the liquid volume of nitrogen at a relative pressure of approximately 0.995 according to the Barrett–Joyner–Halenda (BJH) approach based on desorption data [37].

The NH_3-TPD was carried out on a Belsorp Max (BEL Japan). The samples were degassed at elevated temperature of 100-200 °C for 2 h to remove physisorbed gases prior to the measurement. The temperature was then kept at 200 °C for 2 h while flushed with He gas. NH_3 gas (balanced NH_3, 80% and He, 20%) was introduced at 100 °C for 30 min, then evacuated

Copyright © 2023, ISSN 1978-2993

by helium gas to remove the physisorbed also for 30 min. Finally, temperature programmed desorption was carried out at temperature of 100 – 800 °C and the desorbed NH_3 was monitored by TCD.

The H_2-TPR was performed on a Chemisorb 2750, Micromeritics. The samples were heated at 110 °C for 2 h under N_2 stream with flow rate of 40 ml/min, then cooled to room temperature. Before reduction processes, the line was purged with H_2 (5% Ar gas v/v) for 30 min, then reduced with the same gas (H_2 (5% Ar v/v)) at elevated temperature of 30-700 °C with ramping 10 °C/min. The H_2 uptake was calculated by using calibration curve (H_2 gas; 5% Ar gas v/v, and flow rate of 40 ml/min).

2.2.2 Hydrogenation of LA to GVL

A typical procedure for the catalytic reaction is described as follow: Catalyst (24 mg), LA (2.0 mmol), H_2O (3 mL) as a solvent, and dodecane (0.2 mmol) as an internal standard were placed into a glass reaction tube, fitted inside a stainless-steel reactor of TAIATSU Techno, Japan. After H_2 was introduced into the reactor with an initial H_2 pressure of 30 bars at room temperature (30 °C). After 3 h (180 min), the conversion of LA and the yield of GVL were determined via GC analysis. For reusability test, the used Ru-Sn(3.0)/Nb_2O_5 catalyst was easily separated using either simple centrifugation or filtration in air and dried under vacuum at room temperature, then it was utilized repeatedly without any additional treatments.

2.2.3 Product analysis

Analysis of reactants (LA, aldehydes, ketones, carboxylic acids) and products (GVL, 2-MeTHF, 2-PeOH, and alcohols) was performed on a Perkin Elmer XL-Autosystem equipped with a flame ionization detector and with Restek Rtx® BAC Plus 1 capillary column (30 m, 0.32 mmID, 1.8 mdf). Gas chromatography-mass spectrometry (GC-MS) was performed on a Shimadzu GC-17B equipped with a thermal conductivity detector and with an RT-ßDEXsm capillary column. ^1H and ^{13}C NMR spectra were obtained on a JNM-AL400 spectrometer at 400 MHz; samples were dissolved in chloroform-d_1 or D_2O with TMS as an internal standard. The calibration curve was performed using known concentrations of internal standard, reactants, and products to determine the correct response factors. The conversion of levulinic acid and yield of the products were calculated according to the following equations (Equations (1) and (2)).

$$Conversion = \frac{C_0 - C_t}{C_0} \times 100\% \quad (1)$$

$$Yield = \frac{mol\ product}{introduced\ mol\ reactant\left(C_0\right)} \times 100\% \quad (2)$$

where, C_0 is the introduced mol reactant (levulinic acid) and C_t is the remaining mol reactant, which are all obtained from GC analysis using an internal standard technique.

The turnover frequency (TOF, $mol_{GVL}.mol_{Ru}^{-1}.h^{-1}$) was calculated with high yield of GVL by using Equation (3).

$$TOF\ (h^{-1}) = \frac{Amount\ of\ GVL\ produced\ (mol_{GVL})}{Total\ metal\ Ru\ (mol_{Ru}) \times time\ (h)} \quad (3)$$

Table 1. Results of RT hydrogenation of LA to GVL over various supported ruthenium-based catalysts at low temperature.

Entry	Catalyst	Conversion[a] (%)	Yield[a] (%)		TOF[b]
			GVL	*p*-LA	
1	Ru-Sn(3.0)/Nb_2O_5 (*unred.*)	52	36	16	-
2	Ru-Sn(3.0)/Nb_2O_5 400 °C/H_2	85	85	0	133
3	Ru-Sn(3.0)/Nb_2O_5 500 °C/H_2	98	98	0	306
4[c]		71	71	0	297
5[d]		96	96	0	301
6	Ru-Sn(1.5)/Nb_2O_5 500 °C/H_2	83	83	0	297
7	Ru (5 wt%)/Nb_2O_5	57	29	28	168
8	Sn/Nb_2O_5	-	-	-	-
9	$RuCl_3$	-	-	-	-
10	None	-	-	-	-

Reaction conditions: catalyst (2.4 mg), LA (2.0 mmol), H_2O (3.0 mL), H_2 (30 bar), 30 °C, 3 h. [a]Conversion of LA and Yield of GVL were determined by GC using an internal standard technique. [b]TOF is turnover frequency of GVL formation ($mmol_{GVL}.mol_{Ru}^{-1}.h^{-1}$). [c]At 10 bar H_2. [d]The second reaction run (the recovered catalyst was used without any treatment).

Copyright © 2023, ISSN 1978-2993

3. Results and Discussion

3.1 Hydrogenation of LA over Ru-Sn(x)/Nb_2O_5 Catalyst

In the first set experiments, we conducted the aqueous phase hydrogenation of LA to GVL at low temperature using Ru-Sn/Nb_2O_5 catalysts at 30 °C, 30 bar H_2 for 3 h and the results are summarised in Table 1. Unreduced Ru-Sn(3.0)/Nb_2O_5 catalyst converted 52% of LA to produce 36% GVL and 16% *pseudo*-levulinic acid (*p*-LA) (entry 1). Over pre-educed Ru-Sn(3.0)/Nb_2O_5 400 °C/H_2 catalyst, a remarkably high yield of GVL (85%) was obtained at 85% conversion of LA with the average GVL productivity (TOF) was 133 $mmol_{GVL}.mol_{Ru}^{-1}.h^{-1}$ (entry 2). Further increase in the reduction temperature, Ru-Sn(3.0)/Nb_2O_5 500 °C/H_2 catalyst exhibited the highest yield of GVL (98%) with the average GVL productivity (TOF) of 306 $mmol_{GVL}.mol_{Ru}^{-1}.h^{-1}$ under the same reaction conditions (entry 3). These results indicate that the reduction of catalyst with hydrogen is important to produce highly active and selective bimetallic Ru-Sn catalysts for hydrogenation of LA to GVL.

To clarify the effect of initial H_2 pressure, the reaction was conducted at initial H_2 pressure of 10 bar and LA conversion was significantly decreased to 71% without altering of GVL selectivity (entry 4). The reusability of Ru-Sn(3.0)/Nb_2O_5 500 °C/H_2 was also evaluated and the conversion of LA, selectivity of GVL, and apparent reaction rate showed almost constant after the second reaction run (entry 5). Furthermore, when the amount of Sn was increased (Ru/Sn molar ration of 1.5), the conversion of LA significantly decreased to 83% without the change of GVL selectivity (entry 6). In contrast, the conversion of LA and yield of GVL were 29% and 28%, respectively over unmodified Ru (5wt%)/Nb_2O_5 catalyst (entry 7). This is consistent with the fact that the presence of tin metal in Ru-Sn(x)/Nb_2O_5 catalyst beneficially affected to the activity and selectivity of Ru nanoparticle in the hydrogenation of LA [34] and various carboxylic acids [38]. In addition, Sn/Nb_2O_5 and $RuCl_3$ were inactive for hydrogenation of LA (entries 8-9) and no reaction was observed in absence of catalyst (entry 10).

3.2 Effect of Catalyst Support

To understand the role of support, various supported bimetallic Ru-Sn catalysts were prepared and tested for the hydrogenation of LA to GVL under the same reaction conditions and the results are summarised in Table 2. Five types of supports (*e.g.,* ZrO_2, TiO_2, ZnO, γ–Al_2O_3, and activated charcoal (AC) were employed for the preparation of supported bimetallic Ru-Sn catalysts. Ru-Sn(3.0)/ZnO catalyst converted 96% LA to produce high yield of GVL (96%) (entry 1), which is comparable with the Ru-Sn/Nb_2O_5 catalysts. It has been reported that both Nb_2O_5 and ZnO are typical acidic supports that could play as the Brønsted acid sites, while Ru-Sn or SnO_x could serve as the Lewis acid sites during the hydrogenation of carboxylic acids under aqueous phase reaction [39,40]. To confirm this suggestion, catalytic reaction over Ru-Sn(3.0)/γ–Al_2O_3 catalyst showed quiet high LA conversion (85%), however quite high remained yield of *p*-LA (24%) was observed indicating the effect of acidic support inhibit the reaction of GVL formation (entry 2). In fact, catalytic reaction over monometallic Ru/Nb_2O_5 gave only 57% LA conversion to produce 29% GVL and 28% p-LA (Table 1, entry 7). This result suggested that the high yield of GVL over Ru-Sn/Nb_2O_5 and Ru-Sn/ZnO was mainly due the synergistic action between Ru-Sn or SnO_x species and acidic metal oxide support. Though the precise role of Nb_2O_5 or ZnO as support in is not yet clear, previous reports have showed that the domination of Sn-support and Ru-support are generally known [34]. Strong metal–support interactions in supported Ru–Sn catalysts may hinder the formation of Ru–Sn alloys. It is therefore assumed

Table 2. Results of RT hydrogenation of LA to GVL over Ru-Sn(3.0) catalysts on various supports.

Entry	Catalyst	Conv.[a] (%)	Yield[a] (%)	
			GVL	*p*-LA
1	Ru-Sn(3.0)/ZnO	96	96	0
2	Ru-Sn(3.0)/g-Al_2O_3	85	61	24
3	Ru-Sn(3.0)/TiO_2	47	47	0
4	Ru-Sn(3.0)/ZrO_2	66	66	0
5	Ru-Sn(3.0)/AC	73	73	0

Reaction conditions: catalyst (2.4 mg), LA (2.0 mmol), H_2O (3.0 mL), H_2 (30 bar), 30 °C, 3 h. [a]Conversion of LA and Yield of GVL were determined by GC using an internal standard technique.

Copyright © 2023, ISSN 1978-2993

that Nb_2O_5 or ZnO, as a support material, may provide moderate metal–support interactions to generate the Ru_3Sn_7 alloy, which is the robust and active phase for hydrogenation [41]. Likewise, the second role of Nb_2O_5 or ZnO is supposedly hydrogen supply through hydrogen dissociation on Nb_2O_5 or ZnO and hydrogen spillover from Nb_2O_5 or ZnO to Ru^0 in the Ru–Sn alloy or on isolated ruthenium metal surfaces [42]. As the results, high conversion of LA and high yield of GVL were obtained even more under room temperature. Moreover, other supported Ru-Sn(3.0) catalysts (*e.g.,* Ru-Sn(3.0)/TiO_2, Ru-Sn(3.0)/ZrO_2 and Ru-Sn(3.0)/AC) showed 47-73% conversion of LA (entries 2-5). These results suggest that the unmodified TiO_2, ZrO_2, or AC supported may require more time or temperature reaction to achieve the completed reaction compared to the their modified support as already described in the above introduction. Therefore, it can be concluded that supported Ru-Sn(3.0)/Nb_2O_5 and Ru-Sn(3.0)/ZnO catalysts were the highest activity and selectivity for RT hydrogenation of LA to GVL.

3.3 Role of Solvent

To assess the effect of solvent and initial H_2 pressure on the LA conversion and yield of GVL, the hydrogenation of LA was carried ou in absence of solvent and in various solvents (*e.g.,* 2-propanol, 1,4-dioxane, H_2O/2-propanol and H_2O/1,4-dioxane) the results are also shown in Table 3.

The reaction in the absence of solvent only afforded 19% conversion of LA (19% yield of GVL) even at high H_2 pressure (30 bar) and after 3 h (entry 11). It may be due to the saturation of active site of catalyst by the presence of high concentration of molecular reactant. The use of 2-propanol, 1,4-dioxane, H_2O/2-propanol, and H_2O/1,4-dioxane resulted in quiet low LA conversion of 25%, 29%, 52%, and 40%, respectively (entries 2-5) to yield low amount of GVL. The effectivity of solvents during the hydrogenation reaction is related to their dielectric constant (e). It is found that among the studied solvents, H_2O has the highest dielectric constant of 78.54, which may affect the miscibility of reaction system. Our previous results have also shown that hydrogenation of LA to GVL in the presence of bimetallic Ni-Sn alloy catalyst was effectively occurred in H_2O or its mixture solvents (e.g., H_2O/2-Propanol or H_2O/ethanol or H_2O/methanol) [43,44].

3.4 Substrate Scope

The substrate scope of the Ru-Sn(3.0)/Nb_2O_5 and Ru-Sn(3.0)/ZnO catalysts in the hydro-

Table 3. Results of RT hydrogenation of LA to GVL over Ru-Sn(3.0)/Nb_2O_5 500 °C/H_2 catalyst at RT.

Entry	Solvent	ε^a	Conv.^{b} (%)	Yield^b (%)	
				GVL	*p*-LA
1	Solvent-free	-	19	19	0
2	2-Propanol	18.5	25	15	10
3	1,4-Dioxane	2.21	29	19	0
4	H_2O/2-Propanol	-	52	38	14
5	H_2O/1,4-Dioxane	-	40	30	10

Reaction conditions: catalyst (2.4 mg), LA (2.0 mmol), H_2O (3.0 mL), H_2 (30 bar), 30 °C, 3 h. ^{a}Dielectric constant. ^{b}Conversion of LA and Yield of GVL were determined by GC using an internal standard technique.

Table 4. Results of catalytic hydrogenation of various carboxylic acids, ketones, and aldehydes over Ru-Sn(3.0)/Nb_2O_5 and Ru-Sn(3.0)/ZnO catalysts.

Entry	Substrate	Product	Ru-Sn(3.0)/Nb_2O_5		Ru-Sn(3.0)/ZnO	
			Conv.^{a} (%)	Yield^a (%)	Conv.^{a} (%)	Yield^a (%)
1^b	Dodecanoic acid	n-Dodecanol	82	80	79	78
2	1-Pentenoic acid	1-Pentenol (1-Pentanol)	59	57(2)	61	59(2)
3	Methyl levulinate	γ-Valerolactone	76	76	81	81
4	2-Pentanone	2-Pentanol	83	83	79	79
5	Acetophenone	1-Phenyl ethanol	76	76	81	81
6	Cyclopentanone	Cyclopentanol	78	78	64	64
7^{b,c}	Furfural	Furfuryl alcohol (THFalc)	98	96(2)	93	90(3)
8^c	Furfuryl alcohol	THFalc	11	11	9	9
9^c	2-Methylfuran	Tetrahydromethylfuran	17	17	13	13

Reaction conditions: catalyst (24 mg), substrate (2.0 mmol), 2-propanol or H_2O (3.0 mL), H_2 (30 bar), 3 h, 30-50 °C. ^{a}Conversion of LA and yields were determined by GC using an internal standard technique, ^{b}At 50 °C, ^{c}In 2-propanol.

Copyright © 2023, ISSN 1978-2993

genation of various carboxylic acids, aldehydes, and ketones was examined and the results are summarised in Table 4.

Hydrogenation of aliphatic carboxylic acids such as dodecanoic acid over Ru-Sn(3.0)/Nb_2O_5 catalyst produced 80% yield of n-dodecanol at 82% conversion, while Ru-Sn(3.0)/ZnO catalyst gave 78% yield at 79% conversion at 500 °C, 30 bar H_2 for 3 h, in 1,4-dioxane/H_2O (entry1) [30,45]. Both Ru-Sn(3.0)/Nb_2O_5 and Ru-Sn(3.0)/ZnO catalysts exhibited high selectivity towards unsaturated alcohol (1-pentenol; ~93% selectivity) from hydrogenation of unsaturated 1-pentenoic acid at moderate conversion (59-61%) (entry 2). These results indicate that our Ru-Sn(3.0)/Nb_2O_5 and Ru-Sn(3.0)/ZnO catalysts is active and selective for hydrogenation both C=O and −COOH to corresponding alcohols even under low reaction temperature.

Moreover, hydrogenation of typical ketone 2-pentanone was also examined and afforded 83% 2-pentanol (Ru-Sn(3.0)/Nb_2O_5) and 79% 2-propanol (Ru-Sn(3.0)/ZnO) (entry 4). Acetophenone, a typical and simplest aromatic ketone, was selectively hydrogenated to phenyl ethanol (76-81%) without hydrogenation of the C=C of aromatic ring under current conditions (entry 5). Typical cyclic ketone of cyclopentanone showed higher reactivity over these catalysts as indicated by the high conversion (64-78%) and high yield of cyclic alcohol (entry 6). In addition, hydrogenation of biomass-derived furfural selectively produced furfuryl alcohol and small amount of tetrahydrofurfuryl alcohol (THFalc) with yield of 96% (Ru-Sn(3.0)/Nb_2O_5) and 90% (Ru-Sn(3.0)/ZnO) under the same reaction conditions (entry 7). In contrast, hydrogenation of furfuryl alcohol, and 2-methylfuran in ethanol or H_2O [46,47] produced tetrahydrofurfuryl alcohol (9-11%) (entry 8) or tetrahydromethylfuran(13-17%) (entry 9). These results confirmed that Sn-modified Ru/Nb_2O_5 and Ru/ZnO catalysts showed higher activity towards the hydrogenation of C=O rather than C=C bond in ketones and aldehydes, thus much higher unsaturated alcohols were obtained.

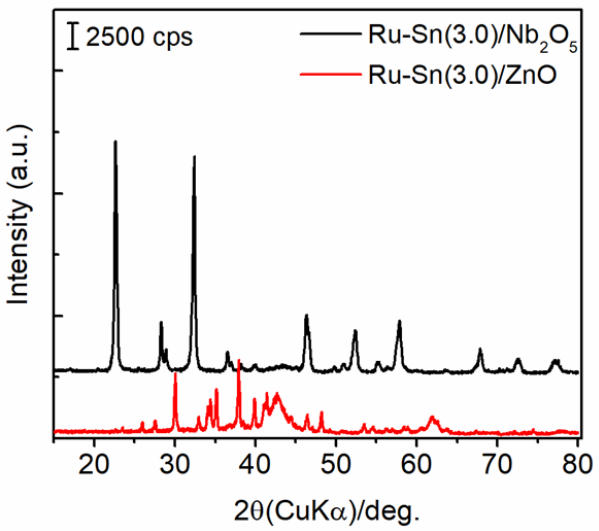

Figure 1. XRD patterns of supported Ru-Sn(3.0)/Nb_2O_5 and Ru-Sn(3.0)/ZnO after reduction with H_2 at 500 °C for 1.5 h.

3.5 Structure-Activity Relationship

To understand the structure-activity relationship both Ru-Sn(3.0)/Nb_2O_5 and Ru-Sn(3.0)/ZnO catalysts were characterized by means of ATR-IR, XRD, N_2 adsorption, H_2 chemisorption, and NH_3-TPD techniques. The physico-chemical properties of the catalysts are summarized in Table 5. Figure 1 shows the XRD patterns of representative supported Ru-Sn catalysts after reduction with H_2 at 500 °C for 1.5 h. The XRD patterns exhibited the main diffraction peaks of support, *c.a.* ZnO or Nb_2O_5, and the presence of ruthenium, tin, or Ru-Sn species are unable to detect by using XRD technique due to the extremely low amount of sample.

As expected, the specific surface area BET (S_{BET}) both catalysts exhibited the low surface area of metal oxide support, indicating the ac-

Table 5. Physico-chemical properties of the synthesised Ru-Sn(3.0)/Nb_2O_5 and Ru-Sn(3.0)/ZnO catalysts.

Entry	Catalyst[a]	S_{BET}[b] ($m^2.g^{-1}$)	H_2 uptake[d] ($mmol.g^{-1}$)	Acidic amount[e] (μmol $NH_3.g^{-1}$)		
				Weak (100-600 °C)	Strong (>600 °C)	Total
1	Ru-Sn(3.0)/Nb_2O_5	58.5	1.56	25	96	121
2	Ru-Sn(3.0)/ZnO	68.8	1.42	95	35	130
3	Ru-Sn(3.0)/ZrO_2	63.4	na	57	0	57
4	Ru-Sn(3.0)/γ-Al_2O_3	132	na	174	45	219

[a]The value in the parenthesis is the Ru/Sn molar ratio. [b]S_{BET} is specific surface areas, determined by N_2 physisorption at 77 K using BET method. [d]The H_2 uptake was derived from H_2-TPR data. [e]Acidity was derived from NH_3-TPD spectra.

Copyright © 2023, ISSN 1978-2993

tive metal (Ru or Ru-Sn) would be dispersed on the outer surface of metal oxide support. It is found that the S_{BET} of each sample was around 58-132 cm^2/g which reflected to the S_{BET} of support. The representative of hydrogen-temperature programmed reduction (H_2-TPR) data of Ru-Sn(3.0)/Nb_2O_5 and Ru-Sn(3.0)/ZnO samples were also summarised in Table 5. The H_2 uptake of Ru-Sn(3.0)/Nb_2O_5 sample was 1.56 $mmol.g^{-1}$, while for Ru-Sn(3.0)/ZnO was 1.42 $mmol.g^{-1}$ (entries 1-2). The surface acidity was determined by using ammonia-temperature programmed desorption (NH_3-TPD) and representative NH_3-TPD spectra for Ru-Sn(3.0)/Nb_2O_5 and Ru-Sn(3.0)/ZnO samples are shown in Figure 2.

The NH_3-TPD profiles were formally divided into three desorption temperature regions to denote two types of acid sites [48,49]: (1) weak to moderate acid sites, ranging from 100 to 600 °C and (2) strong acid sites, ranging from >600 to 900 °C (Table 5). Ru-Sn(3.0)/ZnO sample has a peak at 235 °C and two peaks at 570 °C and 650 °C, which can be attributed to the weak and strong acid sites, respectively. In contrast, Ru-Sn(3.0)/ZnO has desorption peak at 600 °C indicating the presence of strong acid site. A small peak with low intensity was also observed at 475 °C over this sample, which can be attributed to the weak acid sites. The presence of both Lewis and Brønsted acids sites were clarified by using pyridine adsorption and the results are shown in Figure 2(b). The spectra of adsorbed species were obtained after introduction of 1-2 ml pyridine at room temperature, followed by purging with N_2 flow at 50 °C until the spectra were stable. According to the literatures of pyridine adsorption peaks on Sn-containing catalysts [50,51], the bands are assigned in the following way. Pyridinium ion (PyH^+) produced by the reaction of pyridine with Brønsted acid sites (B) shows bands around 1633 cm^{-1} (υ_{8a}). Coordinatively bound pyridines on Lewis acid sites (L) shows bands

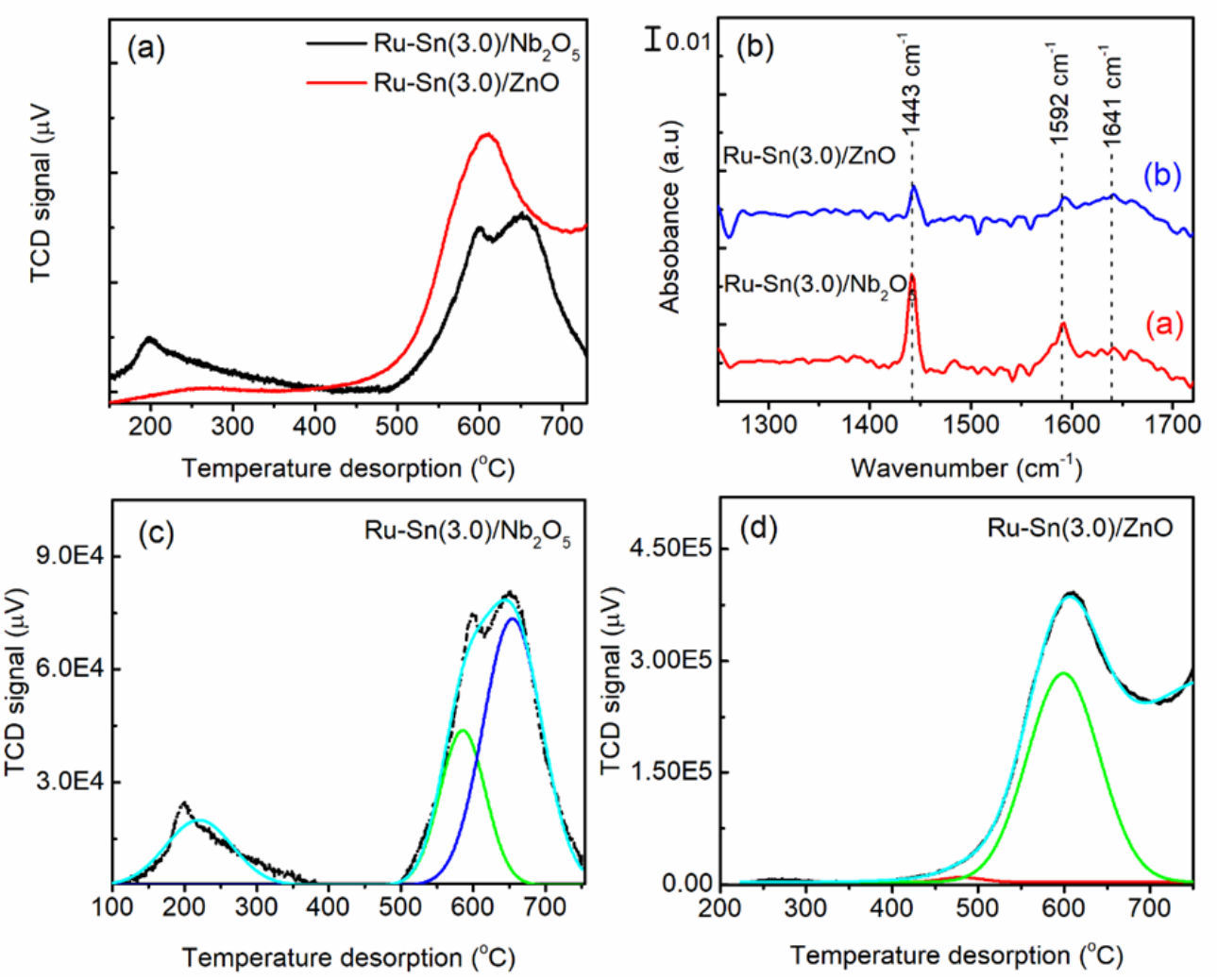

Figure 2. Representative of (a) NH_3-TPD profiles, (b) pyridine adsorption, and deconvoluted NH_3-TPD spectra of (b) Ru-Sn(3.0)/Nb_2O_5 and (c) Ru-Sn(3.0)/ZnO catalysts.

Copyright © 2023, ISSN 1978-2993

around 1445 (υ_{19b}) and 1575 cm^{-1}. Physisorbed or hydrogen-bonded pyridine (H) shows bands around 1437 and 1599 cm^{-1}. The band around 1490 cm^{-1} is common to vibrations due to PyH$^+$ (B) and coordinatively bound pyridine (L) [52]. These results indicate that acid sites of Ru-Sn(3.0)/Nb_2O_5 and Ru-Sn(3.0)/ZnO are both Lewis and Brønsted acidic under the condition in Figure 2(b).

Furthermore, to understand the interaction between the molecular reactant of LA and surfaces of catalyst, the solvent-free reaction (the spectra were recorded according to reaction of entry 1, Table 3) was carried out in the range of 1-3 h and the evolution of two band types at 1700 cm^{-1} (C=O band of LA), and ~1760 cm^{-1} (C=O band of GVL) was monitored by using ATR-IR and the results are shown in Figure 3. A typical absorbance of −COOH of LA was clearly observed at wavenumber of 1700 cm^{-1} after 1 h of reaction. The intensity of n(−COOH) gradually decreased and slightly shifted to higher wavenumber of 1708 cm^{-1} after reaction time of 15 h. The spectra at t = 0 h are the results of LA adsorbed before the reaction at 30 °C after purging with nitrogen gas for 30 min. After hydrogen (30 bar, 30 °C) was introduced, the time-dependence IR spectra was recorded. The time course of the relative amount of the adsorbed LA (area of the C=O stretching band at 1700 cm^{-1}) and the relative amount of GVL formed (area of the C=O stretching band at 1757 cm^{-1}). As seen in Figure 3 shows the IR spectra of representative OH stretching band of H_2O generated from hydrogenation & cyclisation of LA to GVL. The time course of relative amount of generated H_2O intensified as the reaction time was prolonged up to 15 h.

The current results show that the precise design of bimetallic Ru-based catalysts (*e.g.*, the type and amount of second metal (Sn), support) are still challenging to obtain highly active and selective catalyst for room temperature hydrogenation of LA to GVL. The required quite high initial H_2 pressure (30 bar) is challenging in the transformation of various biogenic oxygenated compounds in term of the design of catalyst material. Though, the bimetallic Ru-Sn on ZnO or Nb_2O_5 or even on various studied support in this report showed a great potential for various reactions and further investigation on the fundamental aspect of reaction (kinetic studies, stability and reusability) of type of reaction system (batch of flow) will be a great challenging.

4. Conclusions

Supported bimetallic ruthenium-tin catalysts were examined for the selective hydrogenation of biogenic platform chemicals at low temperature (30-50 °C). Ru-Sn(3.0)/Nb_2O_5 (Ru/Sn = 3.0) that reduced at 500 °C demon-

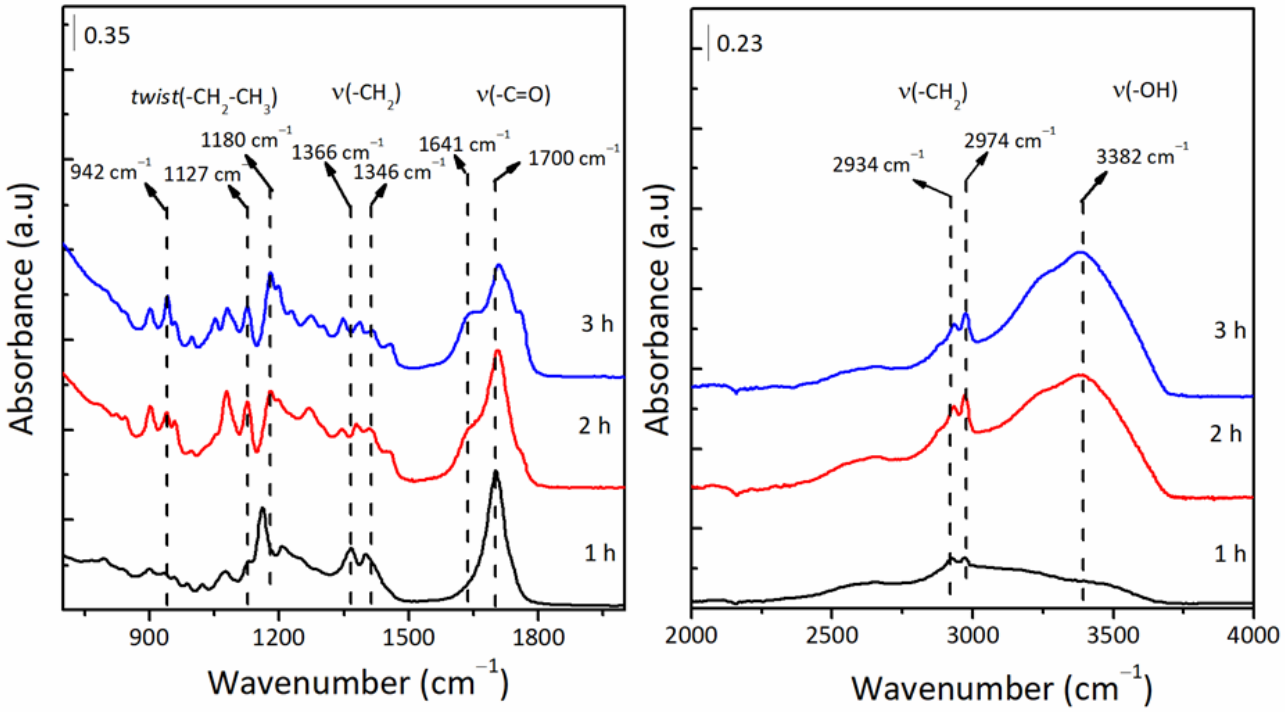

Figure 3. *Ex-situ* ATR-FTIR of solvent free of LA hydrogenation over Ru-Sn(3.0)/Nb_2O_5 catalyst at room temperature. *Reaction conditions:* catalyst (2.4 mg), LA (4.0 mmol), H_2 (30 bar), 30 °C.

Copyright © 2023, ISSN 1978-2993

strated the highest 98% yield of γ–valerolactone at 30 °C, 30 bar H_2 for 3 h. The increase of Sn loading amount (Ru/Sn = 1.5) resulted in decreasing of LA conversion (83%) under the same reaction conditions. Among the studied supported Ru-Sn catalysts, Nb_2O_5 and ZnO supports exhibited better catalytic performances than that other for RT hydrogenation of LA and various biogenic platform chemicals. The high activity and selectivity of both catalysts can be attributed to the synergistic between high dispersion of Ru or Ru-Sn nanoparticles and the presence of Lewis/Brønsted acid sites of the catalyst system. Moreover, the Ru-Sn(3.0)/Nb_2O_5 catalyst was found to be reusable without any significant loss of its activity.

Acknowledgments

The authors acknowledge BPDP Sawit GRS-16 scheme (contract number PRJ-49/2016) and LPDP through *Riset Inovasi Indonesia Maju* tahap 2 (RIIM2) scheme (contract number of 79/IV/KS/11/2022) for financial support (catalyst materials and characterisations). KCS and GKS acknowledge the facilities and technical supports from Advanced Characterisation Laboratories Serpong, National Research and Innovation Agency through E-Layanan Sains (ELSA), *Badan Riset dan Inovasi Nasional* (BRIN). JND acknowledge the Pusat Kolaborasi Riset (PKR) Logam Timah of University of Sultan Ageng Tirtayasa.

CRediT Author Statement

A.S. Azzahra, H.P. Dewi: Formal Analysis, Investigation, ATR-IR study, and Experiment. **R. Rodiansono, I.F. Nata**: Conceptualization, Methodology, Writing-Original draft, Writing-Review & Editing, Supervision. **G.K. Sunnardianto, K.C. Sembiring, J. Jayanuddin**: Writing-Review & Editing, Supervision, Formal Analysis (XRD, NH_3-TPD, H_2-TPR, and N_2-adsorption analyses). All authors have read and agreed to the published version of the manuscript.

References

[1] Kang, S., Fu, J., Zhang, G. (2018). From lignocellulosic biomass to levulinic acid: A review on acid-catalyzed hydrolysis. *Renewable and Sustainable Energy Reviews*, 94, 340–362. DOI: 10.1016/j.rser.2018.06.016.

[2] Han, J., Sen, S.M., Alonso, D.M., Dumesic, J.A., Maravelias, C.T. (2014). A strategy for the simultaneous catalytic conversion of hemicellulose and cellulose from lignocellulosic biomass to liquid transportation fuels. *Green Chemistry*, 16 (2), 653–661. DOI: 10.1039/c3gc41511b.

[3] Machado, G., Leon, S., Santos, F., Lourega, R., Dullius, J., Mollmann, M.E., Eichler, P. (2016). Literature Review on Furfural Production from Lignocellulosic Biomass. *Natural Resources*, 07 (03), 115–129. DOI: 10.4236/nr.2016.73012.

[4] Lange, J.P., van der Heide, E., van Buijtenen, J., Price, R. (2012). Furfural-A promising platform for lignocellulosic biofuels. *ChemSusChem*, 5 (1), 150–166. DOI: 10.1002/cssc.201100648.

[5] Tang, X., Zeng, X., Li, Z., Hu, L., Sun, Y., Liu, S., Lei, T., Lin, L. (2014). Production of γ-valerolactone from lignocellulosic biomass for sustainable fuels and chemicals supply. *Renewable and Sustainable Energy Reviews*, 40, 608–620. DOI: 10.1016/j.rser.2014.07.209.

[6] de Vries, J.G. (2023). Industrial implementation of chemical biomass conversion. *Current Opinion in Green and Sustainable Chemistry*, 39, 100715. DOI: 10.1016/j.cogsc.2022.100715.

[7] Xue, Z., Liu, Q., Wang, J., Mu, T. (2018). Valorization of levulinic acid over non-noble metal catalysts: Challenges and opportunities. *Green Chemistry*, 20 (19), 4391–4408. DOI: 10.1039/c8gc02001a.

[8] Alonso, D.M., Wettstein, S.G., Dumesic, J.A. (2013). Gamma-valerolactone, a sustainable platform molecule derived from lignocellulosic biomass. *Green Chemistry*, 15, 584–595. DOI: 10.1039/C3GC37065H.

[9] Serrano-Ruiz, J.C., West, R.M., Dumesic, J.A. (2010). Catalytic Conversion of Renewable Biomass Resources to Fuels and Chemicals. *Annual Review of Chemical and Biomolecular Engineering*, 1 (1), 79–100. DOI: 10.1146/annurev-chembioeng-073009-100935.

[10] Horváth, I.T., Mehdi, H., Fábos, V., Boda, L., Mika, L.T. (2008). γ-Valerolactone-a sustainable liquid for energy and carbon-based chemicals. *Green Chemistry*, 10 (2), 238–242. DOI: 10.1039/b712863k.

Copyright © 2023, ISSN 1978-2993

[11] Pileidis, F.D., Titirici, M.M. (2016). Levulinic Acid Biorefineries: New Challenges for Efficient Utilization of Biomass. *ChemSusChem*, 9(6), 562–582. DOI: 10.1002/cssc.201501405.

[12] Mascal, M., Dutta, S., Gandarias, I. (2014). Hydrodeoxygenation of the angelica lactone dimer, a cellulose-based feedstock: Simple, high-yield synthesis of branched C7-C10 gasoline-like hydrocarbons. *Angewandte Chemie - International Edition*, 53 (7), 1854–1857. DOI: 10.1002/anie.201308143.

[13] Villa, A., Schiavoni, M., Chan-Thaw, C.E., Fulvio, P.F., Mayes, R.T., Dai, S., More, K.L., Veith, G.M., Prati, L. (2015). Acid-Functionalized Mesoporous Carbon: An Efficient Support for Ruthenium-Catalyzed γ-Valerolactone Production. *ChemSusChem*, 8 (15), 2520–2528. DOI: 10.1002/cssc.201500331.

[14] Rodiansono, R., Azzahra, A.S., Dewi, H.P., Adilina, I.B., Sembiring, K.C. (2023). MoO $_x$-decorated Ru/TiO_2 with a monomeric structure boosts the selective one-pot conversion of levulinic acid to 1,4-pentanediol. *Catalysis Science & Technology*, 13 (15), 4466–4476. DOI: 10.1039/D3CY00544E.

[15] Zhao, Y., Fu, Y., Guo, Q.X. (2012). Production of aromatic hydrocarbons through catalytic pyrolysis of γ-valerolactone from biomass. Bioresource Technology, 114, 740–744. DOI: 10.1016/j.biortech.2012.03.057.

[16] Strádi, A., Molnár, M., Óvári, M., Dibó, G., Richter, F.U., Mika, L.T. (2013). Rhodium-catalyzed hydrogenation of olefins in γ-valerolactone-based ionic liquids. *Green Chemistry*, 15 (7), 1857–1862. DOI: 10.1039/c3gc40360b.

[17] Strappaveccia, G., Luciani, L., Bartollini, E., Marrocchi, A., Pizzo, F., Vaccaro, L. (2015). γ-Valerolactone as an alternative biomass-derived medium for the Sonogashira reaction. *Green Chemistry*, 17 (2), 1071–1076. DOI: 10.1039/c4gc01728e.

[18] Mellmer, M.A., Sanpitakseree, C., Demir, B., Ma, K., Elliott, W.A., Bai, P., Johnson, R.L., Walker, T.W., Shanks, B.H., Rioux, R.M., Neurock, M., Dumesic, J.A. (2019). Effects of chloride ions in acid-catalyzed biomass dehydration reactions in polar aprotic solvents. *Nature Communications*, 10 (1), 1–10. DOI: 10.1038/s41467-019-09090-4.

[19] Nakagawa, Y., Tamura, M., Tomishige, K. (2017). Supported metal catalysts for total hydrogenation of furfural and 5-hydroxymethylfurfural. *Journal of the Japan Petroleum Institute*, 60 (1), 1–9. DOI: 10.1627/jpi.60.1.

[20] Gundeboina, R., Gadasandula, S., Velisoju, V.K., Gutta, N., Kotha, L.R., Aytam, H.P. (2019). Ni-Al-Ti Hydrotalcite Based Catalyst for the Selective Hydrogenation of Biomass-Derived Levulinic Acid to γ-Valerolactone. *ChemistrySelect*, 4 (1), 202–210. DOI: 10.1002/slct.201803407.

[21] Lv, J., Rong, Z., Sun, L., Liu, C., Lu, A.H., Wang, Y., Qu, J. (2018). Catalytic conversion of biomass-derived levulinic acid into alcohols over nanoporous Ru catalyst. *Catalysis Science and Technology*, 8 (4), 975–979. DOI: 10.1039/c7cy01838j.

[22] Li, S., Wang, Y., Yang, Y., Chen, B., Tai, J., Liu, H., Han, B. (2019). Conversion of levulinic acid to γ-valerolactone over ultra-thin TiO_2 nanosheets decorated with ultrasmall Ru nanoparticle catalysts under mild conditions. *Green Chemistry*, 21 (4), 770–774. DOI: 10.1039/c8gc03529f.

[23] Schuette, H.A., Thomas, R.W. (1930). Normal valerolactone. III. Its preparation by the catalytic reduction of levulinic acid with hydrogen in the presence of platinum oxide. *Journal of the American Chemical Society*, 52 (7), 3010–3012. DOI: 10.1021/ja01370a069.

[24] Tan, J., Cui, J., Cui, X., Deng, T., Li, X., Zhu, Y., Li, Y. (2015). Graphene-Modified Ru Nanocatalyst for Low-Temperature Hydrogenation of Carbonyl Groups. *ACS Catalysis*, 5 (12), 7379–7384. DOI: 10.1021/acscatal.5b02170.

[25] Xiao, C., Goh, T.-W.W., Qi, Z., Goes, S., Brashler, K., Perez, C., Huang, W. (2016). Conversion of Levulinic Acid to γ-Valerolactone over Few-Layer Graphene-Supported Ruthenium Catalysts. *ACS Catalysis*, 6 (2), 593–599. DOI: 10.1021/acscatal.5b02673.

[26] Wei, Z., Li, X., Deng, J., Wang, J., Li, H., Wang, Y. (2018). Improved catalytic activity and stability for hydrogenation of levulinic acid by Ru/N-doped hierarchically porous carbon. *Molecular Catalysis*, 448, 100–107. DOI: 10.1016/j.mcat.2018.01.024.

[27] Van Nguyen, C., Matsagar, B.M., Yeh, J.Y., Chiang, W.H., Wu, K.C.W. (2019). MIL-53-NH2-derived carbon-Al2O3 composites supported Ru catalyst for effective hydrogenation of levulinic acid to Γ-valerolactone under ambient conditions. *Molecular Catalysis*, 475(1), 110478. DOI: 10.1016/j.mcat.2019.110478.

[28] Li, S., Wang, Y., Yang, Y., Chen, B., Tai, J., Liu, H., Han, B. (2019). Conversion of levulinic acid to γ-valerolactone over ultra-thin TiO2 nanosheets decorated with ultrasmall Ru nanoparticle catalysts under mild conditions. *Green Chemistry*, 21 (4), 770–774. DOI: 10.1039/c8gc03529f.

Copyright © 2023, ISSN 1978-2993

[29] Zhang, K., Meng, Q., Wu, H., Yuan, T., Han, S., Zhai, J., Zheng, B., Xu, C., Wu, W., He, M., Han, B. (2021). Levulinic acid hydrogenation to γ-valerolactone over single Ru atoms on a TiO2@nitrogen doped carbon support. *Green Chemistry*, 23 (4), 1621–1627. DOI: 10.1039/d0gc04108d.

[30] Ibrahim, I., Riski, M., Rodiansono, R. (2020). The effect of solvent in the hydrogenation of lauric acid to lauryl alcohol using Ru-Fe/TiO2 catalyst. *IOP Conference Series: Materials Science and Engineering*, 980, 012012. DOI: 10.1088/1757-899X/980/1/012012.

[31] Rodiansono, R., Dewi, H.P., Mustikasari, K., Astuti, M.D., Husain, S., Sutomo, S. (2022). Selective hydroconversion of coconut oil-derived lauric acid to alcohol and aliphatic alkane over MoO_x-modified Ru catalysts under mild conditions. *RSC Advances*, 12 (21), 13319–13329. DOI: 10.1039/D2RA02103J.

[32] Ain, N., Rodiansono, R., Mustikasari, K. (2019). Effect of Temperature, Pressure, and Reaction Time on Hydrogenation of Hexadecanoic Acid to 1-Hexadecanol Using a Ru-Sn(3.0)/C Catalyst. *Jurnal Kimia Sains dan Aplikasi*, 22 (4), 112–122. DOI: 10.14710/jksa.22.4.112-122.

[33] Wettstein, S.G., Bond, J.Q., Alonso, D.M., Pham, H.N., Datye, A.K., Dumesic, J.A. (2012). RuSn bimetallic catalysts for selective hydrogenation of levulinic acid to γ-valerolactone. *Applied Catalysis B: Environmental*, 117–118, 321–329. DOI: 10.1016/j.apcatb.2012.01.033.

[34] Vorotnikov, V., Eaton, T.R., Settle, A.E., Orton, K., Wegener, E.C., Yang, C., Miller, J.T., Beckham, G.T., Vardon, D.R. (2019). Inverse Bimetallic RuSn Catalyst for Selective Carboxylic Acid Reduction. *ACS Catalysis*, 9 (12), 11350–11359. DOI: 10.1021/acscatal.9b02726.

[35] Hidajat, M.J., Yun, G.N., Hwang, D.W. (2021). Highly selective and stable ZnO-supported bimetallic RuSn catalyst for the hydrogenation of octanoic acid to octanol. *Molecular Catalysis*, 512, 111770. DOI: 10.1016/j.mcat.2021.111770.

[36] Armarego, W.L.F., Chai, C.L.L. (2009). *Purification of laboratory chemicals*. Elsevier/BH. DOI: 10.1016/C2009-0-26589-5.

[37] Lowell, S., Shields, J.E., Thomas, M.A., Thommes, M. (2004). *Characterization of Porous Solids and Powders: Surface Area, Pore Size and Density*. Dordrecht: Springer Netherlands. DOI: 10.1007/978-1-4020-2303-3.

[38] Zhu, Z., Lu, Z., Li, B., Guo, S. (2006). Characterization of bimetallic Ru-Sn supported catalysts and hydrogenation of 1,4-cyclohexanedicarboxylic acid. *Applied Catalysis A: General*, 302 (2), 208–214. DOI: 10.1016/j.apcata.2006.01.005.

[39] Upare, P.P., Kim, Y., Oh, K.R., Han, S.J., Kim, S.K., Hong, D.Y., Lee, M., Manjunathan, P., Hwang, D.W., Hwang, Y.K. (2021). A Bimetallic Ru_3Sn_7 Nanoalloy on ZnO Catalyst for Selective Conversion of Biomass-Derived Furfural into 1,2-Pentanediol. *ACS Sustainable Chemistry and Engineering*, 9 (51), 17242–17253. DOI: 10.1021/acssuschemeng.1c05322.

[40] Fontana, J., Vignado, C., Jordao, E., Figueiredo, F.C.A., Carvalho, W.A. (2011). Evaluation of some supports to RuSn catalysts applied to dimethyl adipate hydrogenation. *Catalysis Today*, 172 (1), 27–33. DOI: 10.1016/j.cattod.2011.02.030.

[41] Liu, F., Ftouni, J., Bruijnincx, P.C.A., Weckhuysen, B.M. (2019). Phase-Dependent Stability and Substrate-Induced Deactivation by Strong Metal-Support Interaction of Ru/TiO_2 Catalysts for the Hydrogenation of Levulinic Acid. *ChemCatChem*, 11 (8), 2079–2088. DOI: 10.1002/cctc.201802040.

[42] Lee, J.M., Upare, P.P., Chang, J.S., Hwang, Y.K., Lee, J.H., Hwang, D.W., Hong, D.Y., Lee, S.H., Jeong, M.G., Kim, Y.D., Kwon, Y.U. (2014). Direct hydrogenation of biomass-derived butyric acid to n-butanol over a ruthenium-tin bimetallic catalyst. *ChemSusChem*, 7 (11), 2998–3001. DOI: 10.1002/cssc.201402311.

[43] Rodiansono, R., Astuti, M.D., Hara, T., Ichikuni, N., Shimazu, S. (2016). Efficient hydrogenation of levulinic acid in water using a supported Ni-Sn alloy on aluminium hydroxide catalysts. *Catalysis Science and Technology*, 6 (9), 2955–2961. DOI: 10.1039/c5cy01731a.

[44] Tan, J., Cui, J., Deng, T., Cui, X., Ding, G., Zhu, Y., Li, Y. (2015). Water-promoted hydrogenation of levulinic acid to γ-valerolactone on supported ruthenium catalyst. *ChemCatChem*, 7 (3), 508–512. DOI: 10.1002/cctc.201402834.

[45] Damayanti, A.P., Dewi, H.P., Ibrahim, I., Rodiansono, R. (2020). Selective hydrogenation of levulinic acid to gamma-valerolactone using bimetallic Pd-Fe catalyst supported on titanium oxide. *IOP Conference Series: Materials Science and Engineering*, 980, 012013. DOI: 10.1088/1757-899X/980/1/012013.

Copyright © 2023, ISSN 1978-2993

[46] Rodiansono, R., Astuti, M.D., Hara, T., Ichikuni, N., Shimazu, S. (2019). One-pot selective conversion of C5-furan into 1,4-pentanediol over bulk Ni-Sn alloy catalysts in an ethanol/H_2O solvent mixture. *Green Chemistry*, 21 (9), 2307–2315. DOI: 10.1039/c8gc03938k.

[47] Rodiansono, R., Astuti, M.D., Husain, S., Nugroho, A., Sutomo, S. (2019). Selective conversion of 2-methylfuran to 1,4-pentanediol catalyzed by bimetallic Ni-Sn alloy. *Bulletin of Chemical Reaction Engineering & Catalysis*, 14 (3), 529–541. DOI: 10.9767/bcrec.14.3.4347.529-541.

[48] Dumitriu, E., Hulea, V. (2003). Effects of channel structures and acid properties of large-pore zeolites in the liquid-phase tert-butylation of phenol. *Journal of Catalysis*, 218 (2), 249–257. DOI: 10.1016/S0021-9517(03)00159-3.

[49] Khandan, N., Kazemeini, M., Aghaziarati, M. (2008). Determining an optimum catalyst for liquid-phase dehydration of methanol to dimethyl ether. *Applied Catalysis A: General*, 349 (1–2), 6–12. DOI: 10.1016/j.apcata.2008.07.029.

[50] Tututi-Ríos, E., González, H., Cabrera-Munguia, D.A., Gutiérrez-Alejandre, A., Rico, J.L. (2022). Acid properties of Sn-SBA-15 and Sn-SBA-15-$PrSO_3H$ materials and their role on the esterification of oleic acid. *Catalysis Today*, 394–396, 235–246. DOI: 10.1016/j.cattod.2021.09.008.

[51] Rodiansono, Azzahra, A.S., Ansyah, P.R., Husain, S., Shimazu, S. (2023). Rational design for the fabrication of bulk Ni_3Sn_2 alloy catalysts for the synthesis of 1,4-pentanediol from biomass-derived furfural without acidic co-catalysts. *RSC Advances*, 13 (31), 21171–21181. DOI: 10.1039/D3RA03642A.

[52] Tamura, M., Shimizu, K.I., Satsuma, A. (2012). Comprehensive IR study on acid/base properties of metal oxides. *Applied Catalysis A: General*, 433–434, 135–145. DOI: 10.1016/j.apcata.2012.05.008.

Copyright © 2023, ISSN 1978-2993